Journal of the Ceramic Society of Japan 130 [4] 327-330 2022
DOI http://doi.org/10.2109/jcersj2.22009

JCS-Japan

NOTE

A first attempt of automated shrinkage-rate control flash sintering using a current profile without feedback of shrinkage behavior for 8 mol % Y_2O_3-doped ZrO_2

Masao Koike[1], Yuki Ishino[1], Tomoharu Tokunaga[1] and Takahisa Yamamoto[1,†]

[1] Department of Materials Design Innovation Engineering, Nagoya University, Furo-cho, Chikusa-ku, Nagoya 464–8603, Japan

Shrinkage-rate control flash (SCF) sintering is an attractive flash sintering that is modified to densify ceramic green compacts up to high density, which controls electric current to keep shrinkage-rate constant by feedback from shrinkage behavior during a flash state. To build up easier sintering protocol and to realize faster shrinkage-rate, we attempted automated SCF-sintering using the predicted current profile without feedback of the shrinkage behavior. As results, 8YSZ polycrystal with a density of 5.83 g/cm^3 and a grain size of 1.8–4.5 µm could be produced within 10 min during SCF and soaking regimes at the furnace temperature of 870 °C, although the linearity of shrinkage-rate during automated SCF-sintering is degraded from the assumed shrinkage-rate. In order to improve automated SCF-sintering further, a more accurate method of approximating the current profile would be necessary to realize the higher linearity of shrinkage-rate.

Key-words : Flash sintering, SCF, 8YSZ, Zirconia, Fast sintering

[Received January 11, 2022; Accepted January 21, 2022]

Flash sintering has attracted attention to realize instantaneous sintering that can greatly enhance the shrinkage-rate of mainly oxide ceramic green compacts by using electric fields.[1)–3)] The feature of original flash sintering (voltage-to-current flash sintering) is to use the electric power due to a steep current spike, i.e., a flash event, which occurs at threshold furnace temperature during heating green compacts under an electric field.[1)] The enhancement of shrinkage-rate mostly results from Joule heat input due to the flash event.[4)] The steep current spike effective for the enhancement of shrinkage-rate often causes the heterogeneity of microstructure.[5)–8)] For this reason, several methods to control the current spike moderately during a flash event have been reported so far as modified flash sintering.[9)–13)] Among them, shrinkage-rate control flash (SCF) sintering is one of the effective methods, in which the current spike is moderately suppressed to control linear shrinkage-rate at a constant rate.[14)–17)] SCF-sintering is an application of a concept of rate-controlled sintering to flash sintering, which was performed for thermal-sintering in the past.[18),19)] SCF-sintering is superior to the conventional rate-controlled sintering from a viewpoint of controllability of green compact temperature by Joule heat input.[16)] So far, we have succeeded in densifying 3YSZ and 8YSZ polycrystals to relative densities of ~98 % or higher by using this SCF-sintering.[14),15)] However, there are two possible improvements to the present SCF-sintering. The first is the complexity of SCF process, where the linear shrinkage-rate must be measured in-situ and fed back to the current control profile. The other is that the process time for SCF-control is still longer compared to the instantaneous shrinkage achieved by original flash sintering. In order to improve SCF-sintering easier and faster, it is necessary to develop a technique to perform SCF-control only by the predicted current profile without feedback from the shrinkage behaviors.

Thus, in this study, we investigated the possibility of automated SCF-sintering with faster shrinkage-rate only by the usage of the current profile that was predicted from experimental SCF-sintering with slower shrinkage-rate.

A current profile necessary for automated SCF-control was predicted as follows. In original voltage-to-current flash sintering,[1)] the green compact is furnace-heated up to a flash temperature while applying a constant electric field driven by a voltage control mode of a power supply. When the furnace temperature reaches the flash temperature, the current spikes to a current limit of the power supply, and the power supply switches to a current control mode. The magnitude of the current spike depends on the current limit set in the power supply. In contrast, the current limit is set at a smaller value in advance to avoid a large current spike at the flash temperature in SCF-sintering.[14),15)] After the current reaches the initial current limit, the current limit of the power supply is gradually increased so that the shrinkage-rate of green compact becomes constant. To

† Corresponding author: T. Yamamoto; E-mail: yamamoto.takahisa@material.nagoya-u.ac.jp

attempt automated SCF-control, the time transition of the current value (current limit) must be predicted. At first, SCF-sintering was carried out at shrinkage-rate of 120 µm/min, and the current profile was experimentally measured. Then, the obtained current profile was approximated by the following equation,

$$I = A \cdot \ln(t) + (B + Ct) + D \cdot \exp(Et), \qquad (1)$$

where I is current, and A, B, C, D, E are approximating parameters, and t is elapsed time form the onset of SCF-control, respectively. Based on this approximation, we predicted the current profile at faster shrinkage-rate of 720 µm/min, which is too fast rate for controlling experimentally. The current profile at 720 µm/min was calculated by similarly compressing the approximated current profile at 120 to 720 µm/min as a first attempt. An automated SCF-sintering was performed by setting this predicted current profile into a control program of the power supply, in which the current limit values were set at every 5 s interval according to the predicted current profile.

SCF-sintering was conducted as follows. Green compact is furnace-heated at 300 °C/h under a constant electric field of 50 V/cm of 1000 Hz until current reaches initial current limit of 100 mA. When current reaches the current limit, furnace ramp was stopped, and SCF-control was started at the constant furnace temperature. The current during SCF-regime was controlled from initial value of 100 mA to maximum one of 1200 mA. After SCF-regime, the electrical condition was kept further for 5 min as a soaking regime, and then power supply was switched off and sintered compact was furnace-cooled to room temperature.

Green compacts with dimensions of 3.5 × 3.5 × 15 mm^3 were used for these experiments by conventional pressing method including isostatic press at 100 MPa using commercially available 8 mol %Y_2O_3-doped ZrO_2 powder (8YSZ; TZ-8Y, Tosoh Corp., Japan). Platinum sheets were used as the electrode materials and were adhered with Pt paste on both longitudinal faces of the compact. A high-temperature dilatometer (EVO2 TMA8301, Rigaku, Japan) modified to apply an electric field was used for sintering in a controlled electric field.[20)]

The microstructures of the sintered compacts were investigated using scanning electron microscopy (SEM; S-3000H, Hitachi High Technologies, Japan) at an acceleration voltage of 5.0 kV. SEM observation was performed for thermally etched sections at 1250 °C for 1 h after mechanically grinding and polishing the sintered compacts. The density of the sintered compacts was measured using conventional Archimedes method.

Figure 1 shows (a) current profiles, (b) linear shrinkage behaviors, and (c) the time derivative of shrinkage, which were obtained from experimental/automated SCF-sintering at shrinkage-rate of 120 µm/min. In these plots, the data by experimental SCF-sintering is shown with a blue color and by automated SCF-sintering with a red one, respectively. The plots of (c) corresponds to shrinkage-rate variation. The horizontal axis is plotted from the onset time of SCF-regime. In respective SCF-sintering, the furnace temperature

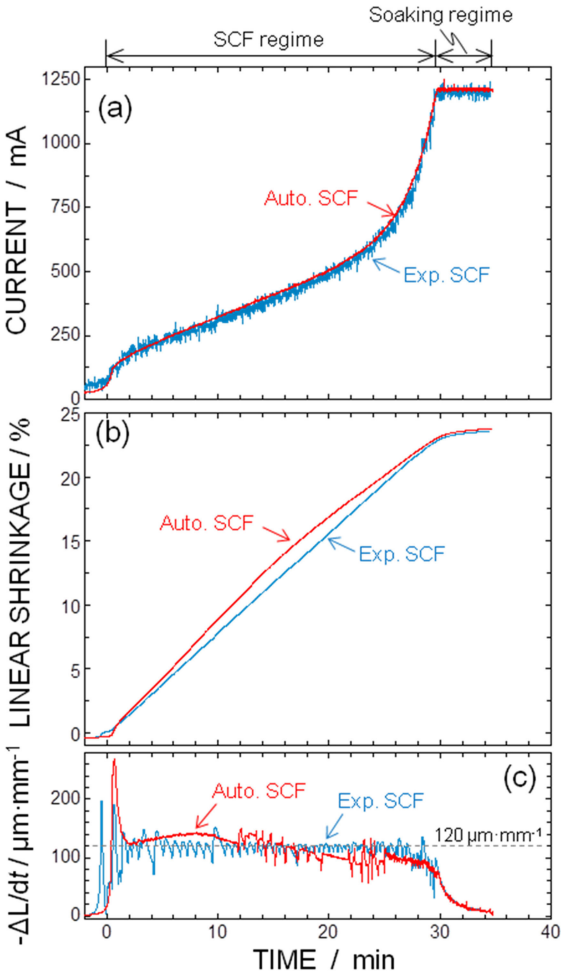

Fig. 1. (a) Current profiles, (b) linear shrinkage behaviors and (c) time derivative of shrinkages ($-\Delta L/dt$) obtained from experimental (blue color) and automated SCF (red color) sintering, which were performed at 50 V/cm of 1000 Hz at the furnace temperature of 870 °C.

at the onset of SCF-control was 870 °C, and SCF-sintering were conducted at this constant furnace temperature.

In experimental SCF-sintering, the current reaches a maximum value of 1200 mA at about 30 min, which corresponds to the end of SCF-regime, and then, the current was kept at 1200 mA about 5 min as a soaking process. The current profile during SCF-regime exhibits a shape like an inversed S-curve to maintain shrinkage-rate at constant, in which the current shows a large increase at the beginning, then the rate of increase decreases, and finally it increases again up to the maximum current value of 1200 mA. The respective behaviors in the inversed S-curve shaped current are approximately dominated by the first, second and third terms of Eq. (1).

Based on this experimental current profile shown with a blue curve of Fig. 1(a), each parameter to approximate this experimental current profile was calculated using Eq. (1) as follows,

$$A = 22.4\,\text{mA},\ B = 112\,\text{mA},\ C = 15\,\text{mA/min},$$
$$D = 6.28 \times 10^{-3}\,\text{mA},\ \text{and}\ E = 0.381/\text{min}.$$

The current profile calculated by Eq. (1) using these parameters is shown with a red curve of Fig. 1(a), which shows in good agreement with the experimental current profile. Automated SCF-sintering was conducted with this current profile, whose shrinkage behavior is shown in Fig. 1(b). The linearity of shrinkage-rate is slightly degraded in automated SCF-sintering comparing that in experimental SCF-sintering, although the deviation of approximated current profile from the experimental one is very small as presented in Fig. 1(a). As shown in the time derivative of shrinkage of Fig. 1(c), shrinkage-rate in automated SCF-sintering varies in a range approximately from 140 to 80 µm/min while almost constant at 120 µm/min in experimental SCF-sintering. It is confirmed that the shrinkage-rate is greatly affected by a slight difference in a current profile, which shows the effectiveness of feedback protocol from shrinkage behavior in previous SCF-sintering. Although the linearity of the shrinkage-rate is slightly inferior, the density of 5.91 g/cm^3 could be obtained by automated SCF-sintering, which is almost the same as the density 5.92 g/cm^3 by experimental SCF-sintering with high linearity of shrinkage-rate. Thus, we consider that the linearity error of shrinkage-rate in automated SCF is acceptable as a first attempt.

Figure 2 shows (a) shrinkage behavior, (b) the time derivative of shrinkage, and (c) current profile obtained by automated SCF-sintering performed with the predicted current profile to assume shrinkage-rate of 720 µm/min that is six times faster of 120 µm/min shown in Fig. 1. This automated SCF-sintering was conducted only by using the predicted current profile without feedback from shrinkage behavior. The current profile shown in Fig. 2(c) is a measured values when a power supply was operated at a current control mode according to the input predicted current profile. The furnace temperature is 870 °C, which is similar to that of Fig. 1.

As shown in Fig. 2(a), shrinkage finally reaches about 23.5 %, which is slightly lower than that of Fig. 1(b). The density of the sintered compact obtained by this automated SCF-sintering was about 5.83 g/cm^3. This density is near theoretical density of 5.97 g/cm^3 of 8YSZ polycrystal.[21] It should be noted that this densification could be achieved within only about 10 min at the furnace temperature of 870 °C. Since the linear shrinkage at the onset of SCF-regime is almost the same as that of the green compact state, i.e., approximately 0 %. The amount of shrinkage during automated SCF-regime was mostly achieved within only 10 min from green compact state.

However, the linearity of shrinkage-rate is largely degraded by the present automated SCF-sintering, in which the shrinkage is roughly linearly controlled until about 4 min, and it increases significantly after 4 min as presented in Fig. 2(a). The detail variation of shrinkage-rate can be confirmed in the plot showing the time derivative of shrinkage in Fig. 2(b), which includes a large surge peak (a red arrow) and a broad peak (near at a blue arrow). The respective peaks are due to a small current surge and an inaccuracy of a predicted current profile, respectively.

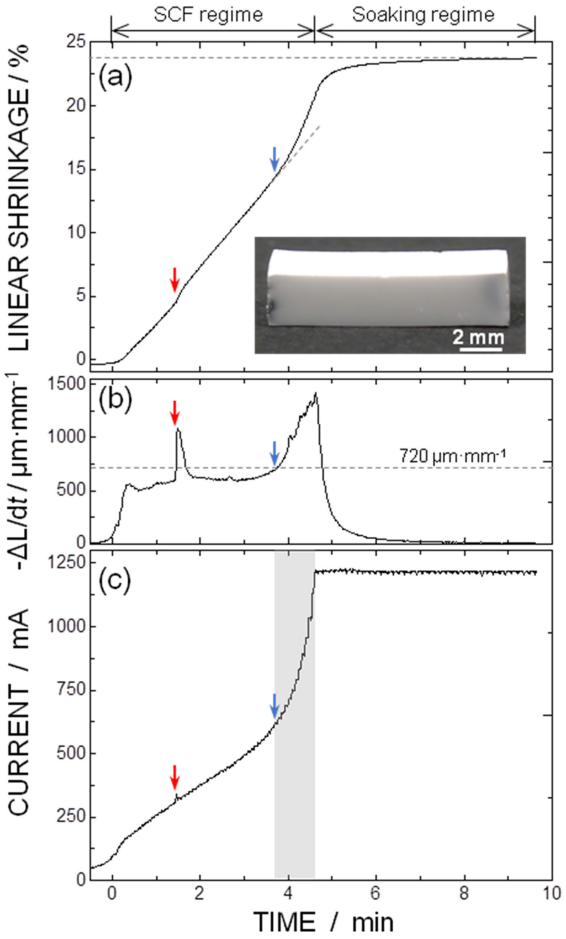

Fig. 2. (a) Linear shrinkage behavior, (b) time derivative of shrinkages ($-\Delta L/dt$), and (c) measured current profile obtained from automated SCF-sintering, which were performed using a predicted current profile without feedback of shrinkage behavior. The inset photograph shows a whole view of automated SCF-sintered 8YSZ polycrystal. The red arrow indicates a timing of an accidental small current surge, and the blue arrow indicated the onset of deviation of non-linearity of shrinkage-rate. The shade in (c) shows the regime of shrinkage-rate deviation due to the inaccuracy of a predicted current profile.

A timing at the large surge peak observed in the time derivative of shrinkage in Fig. 2(b) corresponds to that at a small current surge in a current profile of Fig. 2(c) as indicated by the red arrows. Such a small current surge appears indefinitely during each automated SCF-sintering. This would be due to the indeterminate current path formed accidentally inside the compact due to the increase in a contact area with a neck growth. Although the power supply is driven in a current control mode, the control capability of the power supply is not able to keep up with such sudden current surges. On the other hand, the large deviation of shrinkage-rate from the assumed rate of 720 µm/min is obviously due to the inaccuracy of the predicted current profile, whose regime is indicated with a shade in the current profile of Fig. 2(c). The current increase-rate at the shaded regime of Fig. 2(c) is overestimated to be higher than that of the assumed shrinkage-rate. One reason for this could be that a method to scale a current pro-

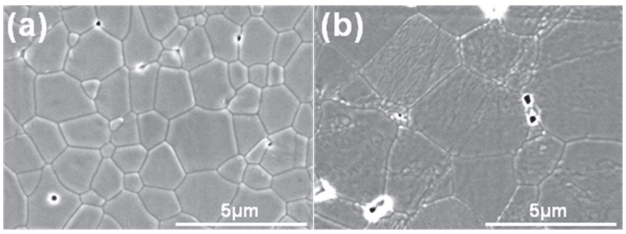

Fig. 3. SEM images taken from thermally etched sections of (a) near surface and (b) center areas in automated SCF-sintered 8YSZ polycrystals.

file shorter from 120 to 720 μm/min is not appropriate. According to the previous SCF-sintering experiments, when shrinkage-rates are increased, the total input power during SCF-regime decreases due to decrease of process time, which may not change linearly with shrinkage-rates. It decreases like-hyperbolically as shrinkage-rate increases.[16] In this study, for the first trial, the current profile at 120 μm/min was approximated by compressing to 720 μm/min in a similar manner. This misalignment leads to an error in the estimation at the shaded regime of current profile in Fig. 2(c). The current profile of this regime is the regime dominated by the third term in Eq. (1) used for current approximation. Thus, it will be necessary to set up variables to scale the shrinkage-rate accurately to develop automated SCF-sintering.

Figure 3 shows microstructure near the surface and the center areas of automated SCF-sintered compact as presented in the inset of Fig. 2(a), respectively. The average grain size in respective areas was approximately 1.8 and 4.5 μm, respectively. In original voltage-to-current flash sintering, Joule heat tends to be more concentrated in the center area of the sintered compact due to the steep current spikes generated at a flash event, which causes a difference in the grain sizes between the respective areas.[8] As presented in Fig. 2(c), the increase-rate of current in a shaded regime was overestimated in the present automated SCF-sintering, which leads to the heterogeneity of the grain size distribution. To develop automated SCF-sintering, the accuracy of the current profile corresponding to the shaded regime of current profile of Fig. 2(c) was revealed to play an important role for the uniformity of grain sizes and achieved density.

In this study, we investigated the possibility for the development of automated SCF-sintering, which realizes SCF-sintering only by controlling current without feedback from shrinkage behavior. The current profile necessary to conduct automated SCF-sintering was approximated by scaling similarly an experimental current profile at slower shrinkage-rate to faster one. As results, 8YSZ polycrystal with a density of 5.83 g/cm^3 and a grain size of 1.8–4.5 μm could be produced within 10 min during SCF and soaking regimes at the furnace temperature of 870 °C. The linearity of shrinkage-rate during automated SCF-sintering is degraded from the assumed shrinkage-rate, which results mainly from inaccuracy of current profile prediction. In addition, the degraded linearity also results in the heterogeneity of grain size distribution. The inaccuracy of the current profile was found to be mainly related to the exponential term in the approximate equation used for this prediction. To further improvement of automated SCF-sintering, a numerical method that can adequately approximate the variable settings involved in the exponential term is necessary.

Acknowledgements This work was supported financially by the Adaptable and Seamless Technology Transfer Program (A-STEP: JPMJTS1617), CREST (JPMJCR1996) from the Japan Science and Technology Agency (JST) and JSPS KAKENHI (Grant Number JP19H05788).

References

1) M. Cologna, B. Rashkova and R. Raj, *J. Am. Ceram. Soc.*, 93, 3556–3559 (2010).
2) M. Yu, S. Grasso, R. Mckinnon, T. Saunders and M. J. Reece, *Adv. Appl. Ceram.*, 116, 24–60 (2017).
3) O. Guillon, R. A. De Souza, T. P. Mishra and W. Rheinheimer, *MRS Bull.*, 46, 52–58 (2021).
4) R. Raj, *J. Eur. Ceram. Soc.*, 32, 2293–2301 (2012).
5) J. C. M'Peko, J. S. C. Francis and R. Raj, *J. Eur. Ceram. Soc.*, 34, 3655–3660 (2014).
6) A. Uehashi, H. Yoshida, T. Tokunaga, K. Sasaki and T. Yamamoto, *J. Ceram. Soc. Jpn.*, 123, 465–468 (2015).
7) W. Qin, J. Yun, A. M. Thron and K. Benthem, *Mater. Manuf. Process.*, 32, 549–556 (2017).
8) J. V. Campos, I. R. Lavagnini, J. G. P. Silva, J. A. Ferreira, R. V. Sousa, R. Mücke, O. Guillon and E. M. J. A. Pallone, *Scripta Mater.*, 186, 1–5 (2020).
9) P. Kumar M K, D. Yadav, J.-M. Lebrun and R. Raj, *J. Am. Ceram. Soc.*, 102, 823–835 (2019).
10) K. H. Christian, H. Charalambous, S. K. Jha and T. Tsakalakos, *J. Eur. Ceram. Soc.*, 40, 436–443 (2020).
11) H. Charalambous, S. K. Jha, K. H. Christian, R. T. Lay and T. Tsakalakos, *J. Eur. Ceram. Soc.*, 38, 3689–3693 (2018).
12) T. P. Mishra, R. R. I. Neto, R. Raj, O. Guillon and M. Bram, *Acta Mater.*, 189, 145–153 (2020).
13) C. A. Grimley, S. Funni, C. Green and E. C. Dickey, *J. Eur. Ceram. Soc.*, 41, 2807–2817 (2021).
14) K. Taguchi, Y. Ishino, T. Tokunaga and T. Yamamoto, *J. Eur. Ceram. Soc.*, 41, 4567–4571 (2021).
15) Y. Ishino, K. Taguchi, M. Koike, T. Tokunaga and T. Yamamoto, *J. Am. Ceram. Soc.*, 104, 4960–4967 (2021).
16) Y. Ishino, K. Taguchi, A. Kodaira, T. Tokunaga and T. Yamamoto, *J. Jpn. Soc. Powder Powder Metall.*, 68, 482–486 (2021).
17) Y. Ishino, K. Taguchi, A. Kodaira, T. Tokunaga and T. Yamamoto, *J. Ceram. Soc. Jpn.*, 129, 551–554 (2021).
18) H. Palmour, III and T. M. Hare, in "Sintering '85", Ed. by G. C. Kucynski, D. P. Uskovic and H. Palmour, Plenum Publishing Corporation, New York (1987) pp. 17–34.
19) O. Abe, *J. Ceram. Soc. Jpn.*, 100, 1196–1199 (1992).
20) N. Morisaki, H. Yoshida, K. Matsui, T. Tokunaga, K. Sasaki and T. Yamamoto, *Appl. Phys. Lett.*, 109, 083104 (2016).
21) R. P. Ingel and D. Lewis, III, *J. Am. Ceram. Soc.*, 69, 325–332 (1986).